Circulation Regimes of Rainfall Anomalies in the African–South Asian Monsoon Belt

UMA S. BHATT

Department of Meteorology, University of Wisconsin, Madison, Wisconsin

(Manuscript received 13 December 1988, in final form 19 April 1989)

ABSTRACT

This study explores the spatial differentiation of climate anomalies and associated circulation mechanisms across the African–South Asian monsoon belt through empirical analyses mainly for the period 1948–83. Observations include surface ship observations in the tropical Atlantic, eastern Pacific, and Indian oceans, and various hydrometeorological and circulation index series, representing the water discharge of the Senegal River (SENEGAL), the rainfall in the West African Sahel (SAHEL), the discharge of rivers in the Nile basin (ROSEIRES, ATBARA), India monsoon rainfall (NIR), and the Southern Oscillation (SO). The field significance of correlation patterns is ascertained through Monte Carlo experiments.

There is a strong correlation of hydrometeorological conditions from Senegal to the Sahel, a decrease from each of these domains eastward to the Nile catchment, and even more so to India. Conversely, correlations are remarkably high between the water discharge of the Nile basin (ROSEIRES, ATBARA) and Indian rainfall (NIR). An SO index is correlated positively with the hydrometeorological conditions throughout the monsoon belt, but most strongly in the East (NIR) and least in the West (SENEGAL).

Correlation analyses for the July–August height of the boreal summer monsoon indicate that abundant rainfall in the western Sahel is, in the Atlantic sector, associated with weak northeast trades and in the western Indian Ocean with low pressure overlying cool surface waters. By comparison, copious river discharge in the eastern portion of the Subsaharan zone coincides with weakened northeast trades over the Atlantic but more pronounced circulation departures in the Indian Ocean sector, consisting of anomalously low pressure, cold surface waters, and abundant cloudiness in the northern Indian Ocean. This ensemble of atmosphere–ocean anomalies is also characteristic of abundant Indian monsoon rainfall. During the positive SO phase, rainfall tends to be relatively abundant throughout the monsoon belt, but most markedly so in the eastern portion of Subsaharan Africa and in India. Overall, the western Sahel shows strongest associations with circulation departures in the tropical Atlantic, whereas the eastern portion of Subsaharan Africa and India are more closely related to the circulation of the Indian Ocean sector.

1. Introduction

The droughts of Subsaharan Africa represent an especially challenging climate problem in terms of the general circulation mechanisms involved and with respect to their severe human impact. It is therefore not surprising that over the past fifteen years they have prompted a series of empirical, theoretical, and modeling investigations [reviews in Hastenrath (1988, pp. 303–309); Druyan (1989)]. In particular, empirical analyses of interannual variability through the early 1970's (Lamb 1978a,b) have documented that abundant summer monsoon rainfall in Subsaharan West Africa is associated with an anomalously far northward position of the near-equatorial trough and embedded confluence zone in the tropical Atlantic sector, that drought years are characterized by broadly inverse departures in large-scale atmospheric and oceanic fields, and that circulation anomaly patterns gradually evolve in the course of the half-year preceding the July–August rainy season peak. General circulation model (GCM) experiments [review in Hastenrath (1988, pp. 304–305)] have examined the possible effect of changes in land surface conditions along the desert fringe and of sea surface temperature (SST) on Sahel rainfall. Thus, in the wake of Charney's (1975) proposition of a "biogeophysical feedback mechanism," a host of papers concentrated on the destruction of plant cover in the Sahel through overgrazing and the consequences on the circulation and climate in this region. Experiments with prescribed SST anomalies were conducted by Palmer (1986), Folland et al. (1986), Druyan (1987, 1988), and Owen and Folland (1988), to explore possible reinforcing factors for rainfall anomalies in the Sahel.

Previous studies of climate variability in the monsoon belt have concentrated on the West African Sahel and India. By comparison, the eastern portion of the Subsaharan zone, and its coherence with West Africa on one hand and with the Indian Ocean sector on the other, has received little attention [review in Kutzbach (1987, pp. 248–252)]. The purpose of the present em-

Corresponding author address: Uma S. Bhatt, Dept. of Meteorology, University of Wisconsin–Madison, 1225 W. Dayton St., Madison, WI 53706.

© 1989 American Meteorological Society

pirical study is to explore the spatial differentiation of climate anomalies and underlying circulation mechanisms across the monsoon belt. This endeavor seems in order, as the causes for the persistence of the current drought regime in the Sahel and its context within the general circulation are not yet understood. The present empirical exploration is also seen as a starting point for judicious GCM experiments directed at the spatial diversity of climate anomalies across the monsoon belt. While seasonal evolutions warrant attention in further work, the present study concentrates on conditions at the height of the boreal summer, when the large-scale circulation reaches an extremum in the annual cycle and when the rainfall activity across the monsoon belt is concentrated.

2. General circulation setting

The monsoon belt, centered around 10°–20°N and extending from the Atlantic across northern Africa, the Indian Ocean and southern Asia to the western extremity of the Pacific, features a complete reversal of lower-tropospheric wind regimes between the boreal winter (November–April) and summer (May–October) semesters [Hastenrath (1988, pp. 107–115, 150–171)]. In boreal winter, the subtropical high pressure axis is located relatively far north, and the northeast monsoon, as part of the planetary-scale northeast trade wind regime, sweeps the area. The near-equatorial trough, in which the airstreams of Northern and Southern hemispheric origins meet, is situated far to the south. Except for limited areas in South Asia, this is the dry season throughout the monsoon belt.

With the heating of the vast Northern hemispheric land masses from May onward, the near-equatorial trough shifts northward, the northeast monsoon retreats, the southeast trades from the Southern Hemisphere cross the equator and reverse to become the southwest monsoon. At the height of the boreal summer around July–August, the near-equatorial trough, and accordingly the poleward limit of the southwest monsoon airstreams, is found at about 20°N over the African continent and even farther north over southern Asia. This is the rainy season throughout the monsoon belt. In the lands along the Gulf of Guinea coast, rainfall maxima occur early and late in the boreal summer semester but a single rainfall peak around July–August prevails across the Sahel belt and most of southern Asia.

3. Observations and basic data processing

The data for this study consist of long-term ship observations in the tropical oceans and various hydrometeorological and circulation index series. Surface ship observations during 1948–83 in the tropical Atlantic, eastern Pacific, and Indian oceans between 30°N and 30°S were obtained from the National Climatic Center at Asheville, North Carolina, for individual months and with a 1-degree square spatial resolution. These formed the basis for a series of climatic atlases (Hastenrath and Lamb 1977, 1978, 1979). Data were later updated to 1983 and compiled into 5-degree square areas. The COADS collection (Oort et al. 1987), which has recently become available, stems largely from the same data source. Elements used here are sea level pressure (SLP), zonal (u) and meridional (v) components of wind, sea surface temperature, and total cloudiness (CLOUD). In the present study, July–August bimonthly values are used, the height of the boreal summer rainy season. Data coverage is most satisfactory for the period 1948–83 used here. As illustrated in Fig. 1, observations are most abundant along the major shipping lanes and scarcest in the southern tropical oceans.

Time series of various indices were compiled to capture the interannual variability of hydrometeorological conditions across the African–South Asian monsoon belt (Fig. 2). For the Senegal river catchment (Figs. 1 and 2), monthly discharge values were seasonalized to yield a 12-month mean value over the interval from May to April, that is, centered on the season of largest discharge. The resulting series of annual values was normalized by dividing by the standard deviation, yielding an index (SENEGAL) of hydrometeorological conditions in the catchment. This index has been used previously in Hastenrath (1976) and Hastenrath et al. (1987). In the same fashion, time series of streamflow

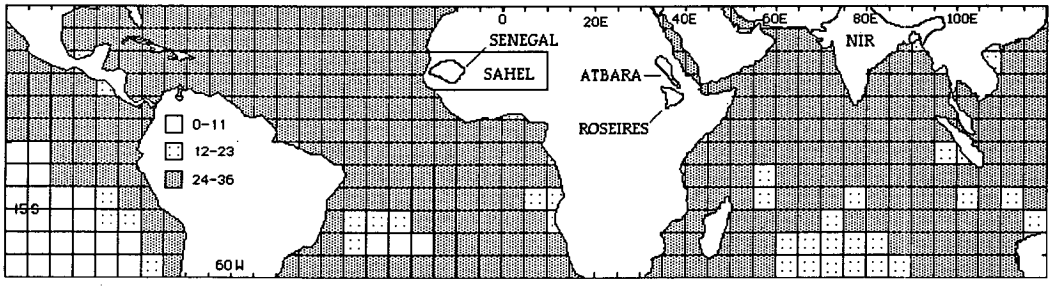

FIG. 1. Orientation map indicating number of July–August seasons during 1948–83 with SST observations in 5 degree blocks, and domains of hydrometeorological index series: Senegal River basin, SENEGAL; Subsaharan West Africa, SAHEL; Blue Nile at Roseires, ROSEIRES; Atbara river basin, ATBARA; all-India rainfall index, NIR.

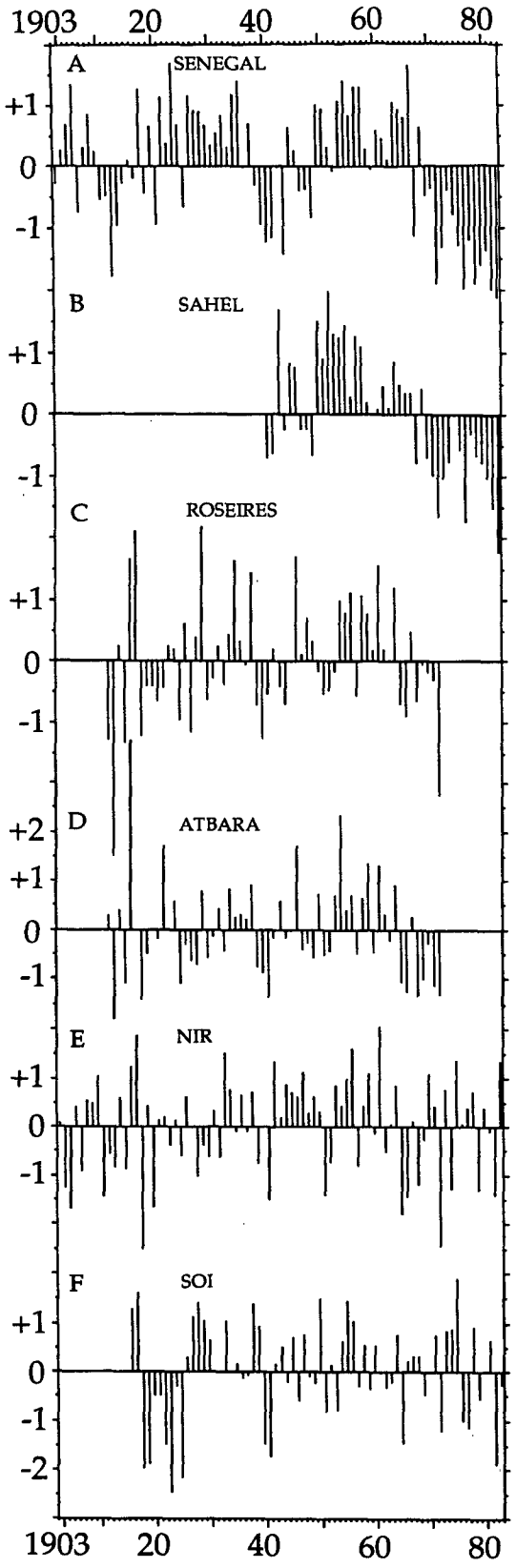

FIG. 2. Time series plots of various hydrometeorological indices for the African-South Asian monsoon belt. (a) SENEGAL—water discharge of Senegal River, 1903–83; (b) SAHEL—rainfall in Subsaharan West Africa, 1941–83; (c) ROSEIRES—Blue Nile river discharge at Roseires, 1912–72; (d) ATBARA—Atbara River discharge, 1912–72; (e) NIR—all-India rainfall index, 1903–83; (f) SOI—SO index of July–August, 1916–83.

indices were constructed for the Blue Nile at Roseires and for the River Atbara, both with seasonalization from April to March. The ROSEIRES and ATBARA indices (Figs. 1 and 2) are based on discharge values to 1972 contained in Shahin (1985, pp. 515–516, 523–524). The SENEGAL, ROSEIRES, and ATBARA river index series describe the hydrometeorological conditions at the western versus the eastern extremities of the Subsaharan zone. These are complemented by the rainfall index series SAHEL (Figs. 1 and 2) compiled by Lamb (1985) from the April–October precipitation at 20 stations across Subsaharan West Africa. Composite series for various Subsaharan domains have also been compiled by Nicholson (1985) and others. The Indian summer monsoon rainfall is represented by an all-India index NIR (Figs. 1 and 2), prepared by Mooley and Parthasarathy (1984) as an area-weighted average of June–September precipitation at 306 stations. For the Southern Oscillation index (SOI), the Tahiti (18°S, 150°W) minus Darwin (12°S, 131°W) pressure difference, normalized by the standard deviation, was used (see Fig. 2).

4. Methods

Correlation coefficients were calculated between various hydrometeorological and circulation index series and atmospheric and oceanic fields in July–August, for the periods 1948–83 and 1948–72. Excluded were 5-degree blocks with data missing for either July or August in 7 or more of the total 36 years and 5 or more of the total 25 years, respectively.

In addition, the regression coefficient b in the regression equation

$$\text{SLP} = a + b \times \text{INDEX}$$

was calculated for all five-degree blocks and mapped. These maps, not reproduced here, in conjunction with the correlation charts serve to ascertain spatial patterns of pressure gradients.

In the significance testing of the correlations, two levels are distinguished. The *local* significance was assessed using a two-tailed t-test at the 5 percent level (Abramowitz and Stegun 1964, p. 990) and accounting for the reduction of effective degrees of freedom due to persistence using the method described by Quenouille (1952, p. 168). The *field* significance of correlation patterns was ascertained by Monte Carlo simulations similar to those described by Livezey and Chen (1983). Of a total number N_t of individual correlations, N will reach local significance at the 5 percent level. Field significance at the 5 percent level is attained when

N exceeds N^*, where N^* is the 95th percentile of the number of locally significant correlations in a field correlated with a random series with the same statistical characteristics as the original INDEX series.

The field significance testing procedure consists of two steps. In the first step, no spatial interdependence is assumed. Then N^* is equal to the 95th percentile of the binomial distribution with N trials and success probability p = 0.05 (Livezey and Chen 1983). If N does not exceed N^* the pattern does not possess field significance at the 5 percent level, and no further significance testing is done. Otherwise we proceed to the second step, in which the spatial interdependence within the field is accounted for. The original INDEX series is randomly rearranged producing a random series with statistical properties identical to the original INDEX. In 200 Monte Carlo experiments, such randomly rearranged series are correlated with the various oceanic fields. These experiments produce 200 values of the numbers N_{mc} of locally significant correlations. When N is greater than the 95 percentile N^*_{mc} of the empirically determined N_{mc}'s, the pattern is considered to possess field significance at the 5 percent level. Note that this field significance testing method does not take spatial position of the blocks that are significant into account. This field significance testing procedure was applied to the combined Atlantic and eastern Pacific oceans and separately to the Indian Ocean.

5. Interannual variability of monsoon rainfall

Throughout the monsoon belt, from the Atlantic coast of Africa to the Indian Ocean sector, rainfall has varied substantially from year to year, as well as over decadal time scales. This is illustrated in Fig. 2, which indicates a considerable coherence of hydrometeorological anomalies throughout the monsoon belt, contained broadly between 10° and 20°N (Fig. 1). In particular, variations of SENEGAL parallel closely the West African rainfall index SAHEL, while similarities with the discharge fluctuations in the Nile basin (ROSEIRES, ATBARA) are less conspicuous. The latter, however, parallel remarkably the vagaries of Indian monsoon rainfall, NIR. For comparison, Fig. 2 also contains a plot of SOI for July–August. For the positive Southern Oscillation (SO) phase, defined by anomalously high/low pressure at Tahiti/Darwin, monsoon rainfall tends to be abundant, but rather deficient in the negative SO phase [reviews in Hastenrath (1988, pp. 284–286); Ropelewski and Halpert (1989)]. Figure 2 suggests, however, that these anomalies may be less prominent in the western than the eastern extremity of the monsoon belt.

The visual impression of associations obtained from Fig. 2 is substantiated quantitatively in Table 1. A strong correlation of hydrometeorological conditions exists between SENEGAL and SAHEL, and a decrease from either of these domains eastward to the Nile catchment (ROSEIRES, ATBARA), and even more so to India (NIR). Conversely, correlations are remarkably high between the water discharge of the Nile basin (ROSEIRES, ATBARA) and Indian rainfall (NIR). It is further noteworthy that SOI is correlated positively with the hydrometeorological conditions throughout the monsoon belt, but most strongly in the East (NIR) and least in the West (SENEGAL).

TABLE 1. Correlation coefficients in hundredths between hydrometeorological indices (see Fig. 2 for explanation of indices and Fig. 1 for locations) for (a) 1948–72; (b) 1948–83; (c) 1916–83. One and two asterisks indicate significance at the 5 and 1 percent levels, respectively. In the significance testing of correlation coefficients, Quenouille's (1952, p. 168) method was used to account for the reduction of the effective number of degrees of freedom due to persistence.

1948–1972

	SAHEL	ROSEIRES	ATBARA	NIR	SOI
SENEGAL	+77**	+49*	+47*	+23	+35
SAHEL		+31	+48*	+14	+27
ROSEIRES			+77**	+84**	+50*
ATBARA				+69**	+37
NIR					+51**

1948–1983

	SAHEL	NIR	SOI
SENEGAL	+86**	+10	+30
SAHEL		+6	+29
NIR			+48**

1916–1972

	ROSEIRES	ATBARA	NIR	SOI
SENEGAL	+29*	+30*	−1	+19
ROSEIRES		+67**	+59**	+47**
ATBARA			+55**	+30*
NIR				+45**

6. Correlation analysis of atmospheric and oceanic fields

The time series of hydrometeorological and circulation indices (Fig. 2; Table 1) discussed in the preceding section indicate a considerable coherence of rainfall anomalies throughout the monsoon belt, but also distinct differences between its western and eastern extremities. The objective of the present section is to explore the circulation departure patterns associated with rainfall anomalies in various portions of the monsoon belt. While the drought regimes of Subsaharan West Africa and of India have been studied extensively, anomalies in the eastern part of Subsaharan West Africa, in particular the Nile basin, have received little attention. Accordingly, rainfall variability in this region is of particular interest, especially its behavior with respect to the well-documented variability to the west (Sahel) and the east (India). Unfortunately, hydrometeorological series for the Nile basin are presently available only until 1972. Therefore, analyses were not only performed for the longer 1948–83 period for SENEGAL, SAHEL, NIR, but also for the 1948–72 period, so as to allow additional comparison with the

results for the Nile basin (ROSEIRES, ATBARA). In the following these domains are now discussed proceeding from west to east.

a. *Senegal catchment*

Figure 3 presents the maps of correlation between SENEGAL and the indicated atmospheric and oceanic fields in the eastern Pacific, Atlantic, and Indian oceans for the years 1948–83. Field significance is reached for SLP, v, and CLOUD, in the eastern Pacific–Atlantic and for v and SST in the Indian Ocean.

Concerning the Pacific–Atlantic domain, SLP correlations (Fig. 3a) are positive in the eastern Pacific, but negative in the North Atlantic between approximately 15 and 25°N. The pressure regression coefficient (not shown here) is also largest in this zone, located between the axis of the North Atlantic subtropical high in the north and the long-term position of the near-equatorial low pressure trough in the south (Hastenrath and Lamb 1977, charts 8 and 9). Negative correlation coefficients together with the largest pressure regression coefficients in this zone mean that, for abundant Senegal discharge, pressure is reduced more strongly in this zone than in the vicinity of the near-equatorial trough to the south. In other words, the meridional pressure gradient is reduced. The pressure regression map and the SLP correlation map together indicate that abundant Senegal discharge tends to be observed concurrently with weakened southward pressure gradients to the north of the near-equatorial trough. In agreement with the SLP map are the largely positive correlations with the zonal and meridional wind components over the North Atlantic (Figs. 3b and 3c), which suggest reduced North Atlantic trades for abundant Senegal discharge. The SST correlation map (Fig. 3d) is characterized by positive values in the North Atlantic, contrasting with negative values in the South Atlantic, consistent with earlier findings (Lamb 1978a,b; Hastenrath 1978; Lough 1986; Hastenrath et al. 1987). The CLOUD correlation map (Fig. 3e) is indistinct. The patterns displayed by the maps in Figs. 3a–e are in good agreement with previous studies [review in Hastenrath (1988, pp. 303–309)].

In the Indian Ocean SLP (Fig. 3a) and u (Fig. 3b) patterns of correlation are indistinct and not field significant. The field significant v correlation pattern (Fig. 3c) indicates that weakened southerlies accompany abundant Senegal River discharge. The map of SST correlations (Fig. 3d), which is field significant, displays strong negative values in the western Indian Ocean. The CLOUD (Fig. 3e) correlation pattern, which is not field significant in the Indian Ocean, is indistinct overall.

Correlation fields for SENEGAL were also constructed for the time period 1948–72. In the Atlantic–eastern Pacific sector are no substantial differences between the two time intervals, except that fewer 5 degree blocks were locally significant for the shorter time period. For the Indian Ocean, the correlation patterns for the shorter time period were indistinct.

In summary, abundant Senegal river discharge is characterized in the Atlantic by reduced northeast trades, and in the Indian Ocean by anomalously cold surface waters and weakened southerly monsoon flow.

Maps of correlations between the hydrometeorological index series SAHEL and atmospheric and oceanic fields are similar to those for SENEGAL (Fig. 3) and are not reproduced here. The SAHEL maps reach field significance in the tropical Atlantic and eastern Pacific for SLP and u, and in the Indian Ocean for v and SST. In brief, abundant western Sahel rainy seasons are characterized in the Atlantic by decreased northeast trades. These features are consistent with the results for SENEGAL and also agree with various earlier studies (Lamb 1978a,b; Hastenrath et al. 1987; Wolter 1989). The Indian Ocean patterns, though less pronounced, do indicate anomalously cool surface waters and weakened southerly flow during copious rainy seasons in the western Sahel.

b. *Nile basin*

Figure 4 contains maps of correlation between an index of Blue Nile river discharge (ROSEIRES) and SLP, u, v, SST, and CLOUD. Field significance is reached in the tropical Atlantic–eastern Pacific for SLP, SST, and CLOUD, and in the Indian Ocean for SLP and CLOUD.

The SLP correlation map (Fig. 4a) features negative values in the North Atlantic, contrasting with strongly positive ones in the eastern Pacific and much of the south Atlantic. The pressure regression map (not reproduced here) shows negative/positive coefficients in the tropical North/South Atlantic. From considerations similar to those in section 6a, this is tantamount to weaker meridional pressure gradients. Consistent with this, the u and v correlation patterns (Figs. 4b and 4c), though not field significant, indicate that copious rainfall in the Blue Nile catchment tends to coincide with reduced North Atlantic trades. The SST correlation map (Fig. 4d) is field significant and contains a large region of negative values in the eastern Pacific, a positive area at 15°N near the west African coast, and negative correlations in the South Atlantic. The field significant CLOUD correlation map (Fig. 4e) indicates that abundant Blue Nile discharge is observed when enhanced cloudiness in the eastern Pacific and clear skies in the western Atlantic occur, although less markedly than for SENEGAL or SAHEL.

The Indian Ocean SLP correlation pattern (Fig. 4a) is field significant and contains a large block of negative correlations in the Arabian Sea. The pressure regression map (not shown here) contains large negative values over the Arabian Sea. From considerations similar to those stated earlier, this corresponds to stronger northward pressure gradients. Consistent with this, the u and v correlation maps (Figs. 4b and 4c), neither of which

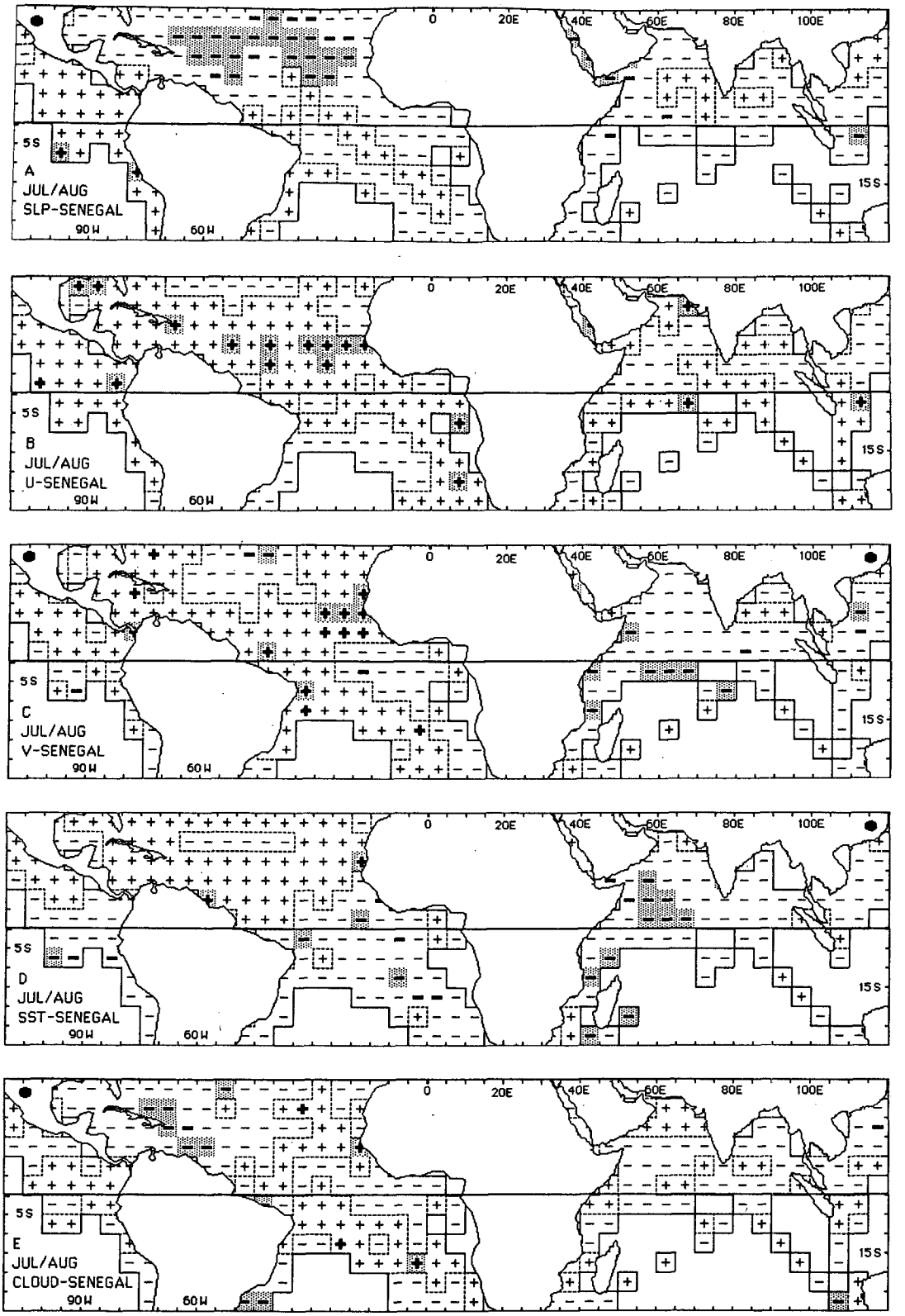

FIG. 3. Patterns of correlation between an index of Senegal River discharge (SENEGAL) and July/August values of indicated elements during 1948–83: (a) sea level pressure SLP, (b) zonal u, and (c) meridional wind component v, (d) sea surface temperature SST, and (e) cloudiness CLOUD. Plus and minus signs denote the sign of the correlation, shading absolute values greater than 0.4, and bold signs indicate *local* significance at the 5 percent level. Quenouille's (1952, p. 168) formulation was used to account for the reduction of the effective temporal degrees of freedom due to persistence. Blank areas indicate blocks with less than 29 years of data. *Field* significance at the 5 percent level, as determined by Monte Carlo experiments, is indicated by dots, in the northwestern corner of the map for the Pacific–Atlantic domain, and in the northeastern corner for the Indian Ocean.

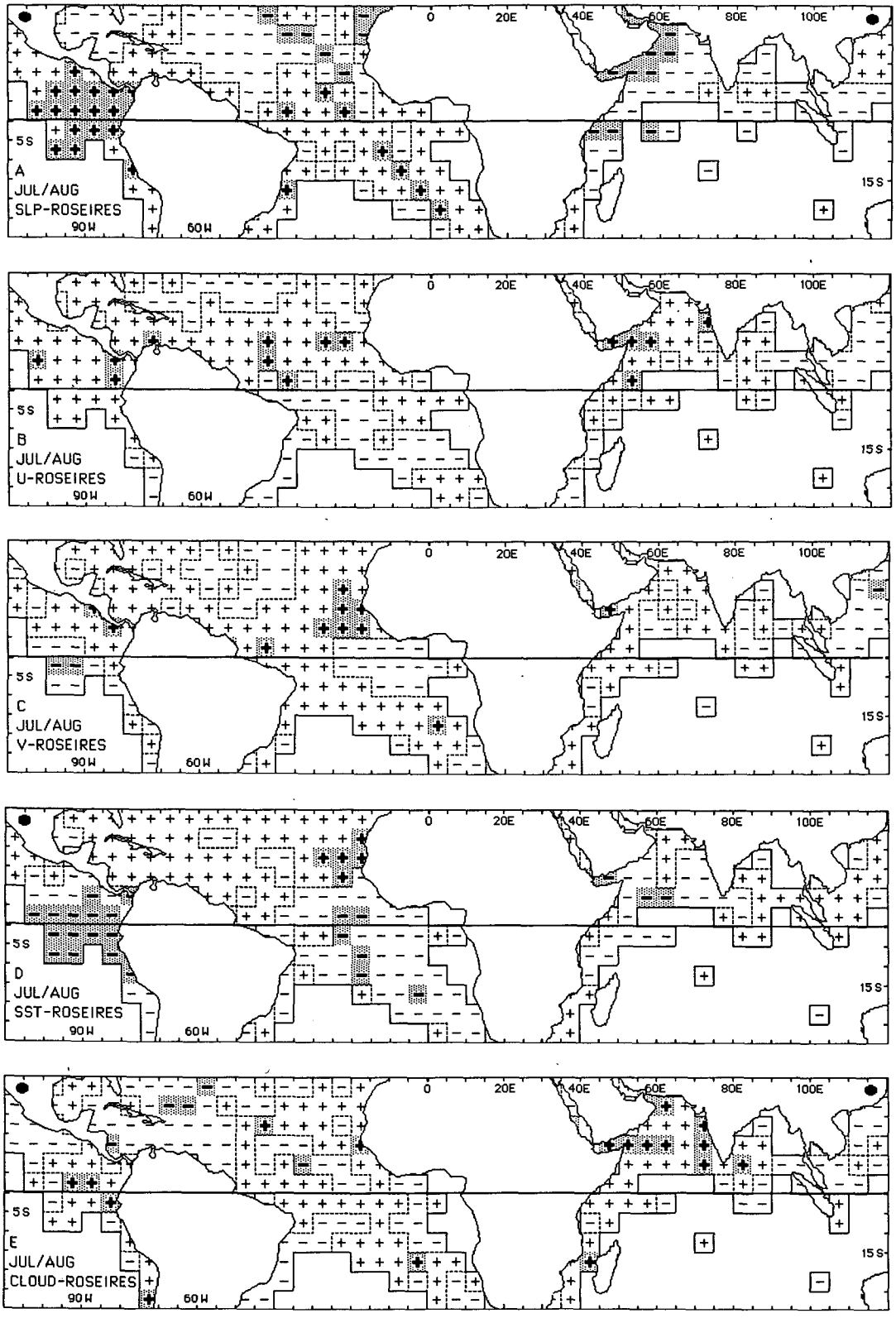

FIG. 4. As in Fig. 3 except for ROSEIRES, period 1948–72. Blank areas indicate blocks with less than 20 years of data.

is field significant, suggest abundant Blue Nile discharge coincides with enhanced southwesterlies in the western Arabian Sea sector. The SST (Fig. 4d) correlation map is not field significant. The CLOUD (Fig. 4e) correlation map contains positive correlations in the western Indian Ocean indicating enhanced cloudiness during abundant Blue Nile discharge.

In summary, during abundant Blue Nile discharge the eastern Pacific features anomalously high pressure, overlying cool surface waters and enhanced cloudiness, all common to the positive SO phase. The positive CLOUD correlations reflect the persistent stratus deck characteristic of the positive SO phase, contrasting with the convective cloudiness typical of El Niño. Abundant Blue Nile discharge is characterized in the Atlantic by decreased northeast trades, resembling the general circulation setting associated with abundant Senegal River discharge or copious Western Sahel rainfall. The Indian Ocean is characterized by anomalously low pressure, generally cool surface waters, and abundant cloudiness when Blue Nile discharge is high. The patterns in the Indian Ocean associated with abundant Blue Nile discharge are similar but stronger than those accompanying copious Senegal River discharge or abundant western Sahel rainfall. Correlation patterns for the period 1948–72 for the River Atbara (ATBARA) are largely similar to those found in the ROSEIRES analysis and are therefore not detailed here.

c. *India*

Maps of correlation between the all-India rainfall index (NIR) and SLP, u, v, SST, and CLOUD are presented in Fig. 5. Field significance is reached only in the Indian Ocean for SLP and CLOUD.

Concerning the Pacific–Atlantic sector, the SLP correlation map is characterized by mainly negative values (Fig. 5a) in the North Atlantic Ocean and by positive values in the southeast Atlantic and eastern Pacific. The u and v correlation maps (Figs. 5b and 5c), neither of which is field significant, contain positive values in the Atlantic and eastern Pacific. The SST correlation map (Fig. 5d) contains negative values in the eastern Pacific. The CLOUD correlation pattern (Fig. 5e) is characterized by positive values in the eastern Pacific. None of the correlations maps reach field significance for the 1948–83 period in the eastern Pacific–Atlantic domain.

The Indian Ocean SLP map of correlation (Fig. 5a) is field significant and displays mainly negative values. The u and v correlation maps (Figs. 5b and 5c), neither of which is field significant, display positive values in the western Indian Ocean. The SST correlation map (Fig. 5d) (not field significant) contains negative values in the western Indian Ocean, which is consistent with previous results [review in Hastenrath (1988, pp. 289–291)]. The field significant CLOUD (Fig. 5e) map is characterized by positive values in the western portion of the Indian Ocean. The correlation maps indicate a tendency for abundant rainfall in India when anomalously low pressure and increased cloudiness in the western Indian Ocean are observed.

Of the maps produced by the analysis for the shorter period 1948–72, SLP and CLOUD are field significant in the Indian Ocean, similar to the maps obtained for 1948–83. Recalling that in the Atlantic none of the maps are field significant for 1948–83, it is interesting to note that in the analysis for 1948–72 the correlation patterns are similar to those for the longer period and field significance is reached for SLP, v, and SST.

In summary, abundant Indian rainfall is associated in the eastern Pacific with high pressure overlying cold surface waters, a characteristic of the positive SO phase; in the Atlantic with no distinct patterns; and in the western Indian Ocean by anomalously low pressure and enhanced cloudiness. These results are consistent with various earlier studies [review in Hastenrath (1988, p. 283–292)].

d. *Southern Oscillation*

Figure 6 presents maps containing correlations between SOI and SLP, u, v, SST, and CLOUD. Field significance is reached for all of the maps in the Pacific–Atlantic domain and for SLP, v, SST, and CLOUD in the Indian Ocean.

Concerning the Pacific–Atlantic domain, the SLP correlation pattern (Fig. 6a) contains negative values in the Atlantic and positive values in the eastern Pacific. The pressure regression coefficient map (not shown here) contains the smallest negative values in the North Atlantic and positive ones throughout the eastern Pacific, displaying a maximum at 0°–5°N with values decreasing northward. From considerations similar to those earlier this implies a steepened northward pressure gradient in the zone 0°–10°N. Together the SLP and regression coefficient maps indicate for the positive SO phase a more poleward position of the near-equatorial low pressure trough in the eastern Pacific. The u correlation map (Fig. 6b) is characterized by positive values in the western Atlantic and eastern Pacific north of the equator, and negative values in the southeast Atlantic. The map of correlations of v with SOI (Fig. 6c) contains positive values north of the equator in the eastern Pacific and western Atlantic, and negative values between 0° and 10°S in the eastern Pacific and much of the eastern equatorial Atlantic. Consistent with the SLP and pressure regression maps, the wind correlation fields indicate weakened northeast trades and enhanced cross-equatorial flow between 0°–10°N in the eastern Pacific. The SST correlation map (Fig. 6d) is characterized by negative values in the eastern Pacific and North Atlantic, and positive values in the South Atlantic. Figure 6e, depicting the correlation patterns of CLOUD, indicates enhanced cloudiness in the eastern Pacific and in the Atlantic near-equatorial trough zone during the positive SO phase.

The Indian Ocean SLP correlation pattern (Fig. 6a)

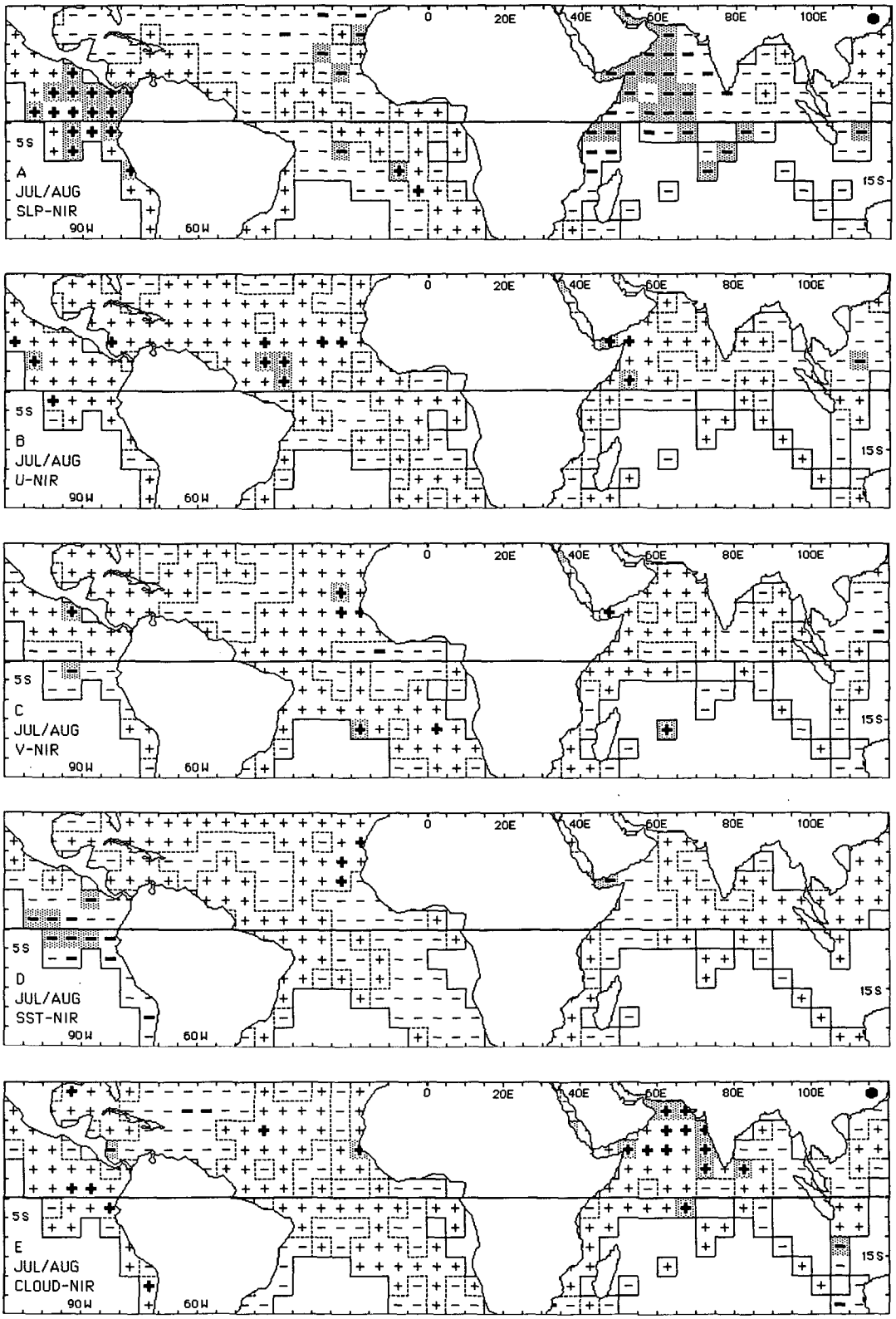

FIG. 5. As in Fig. 3 except for NIR, period 1948–83.

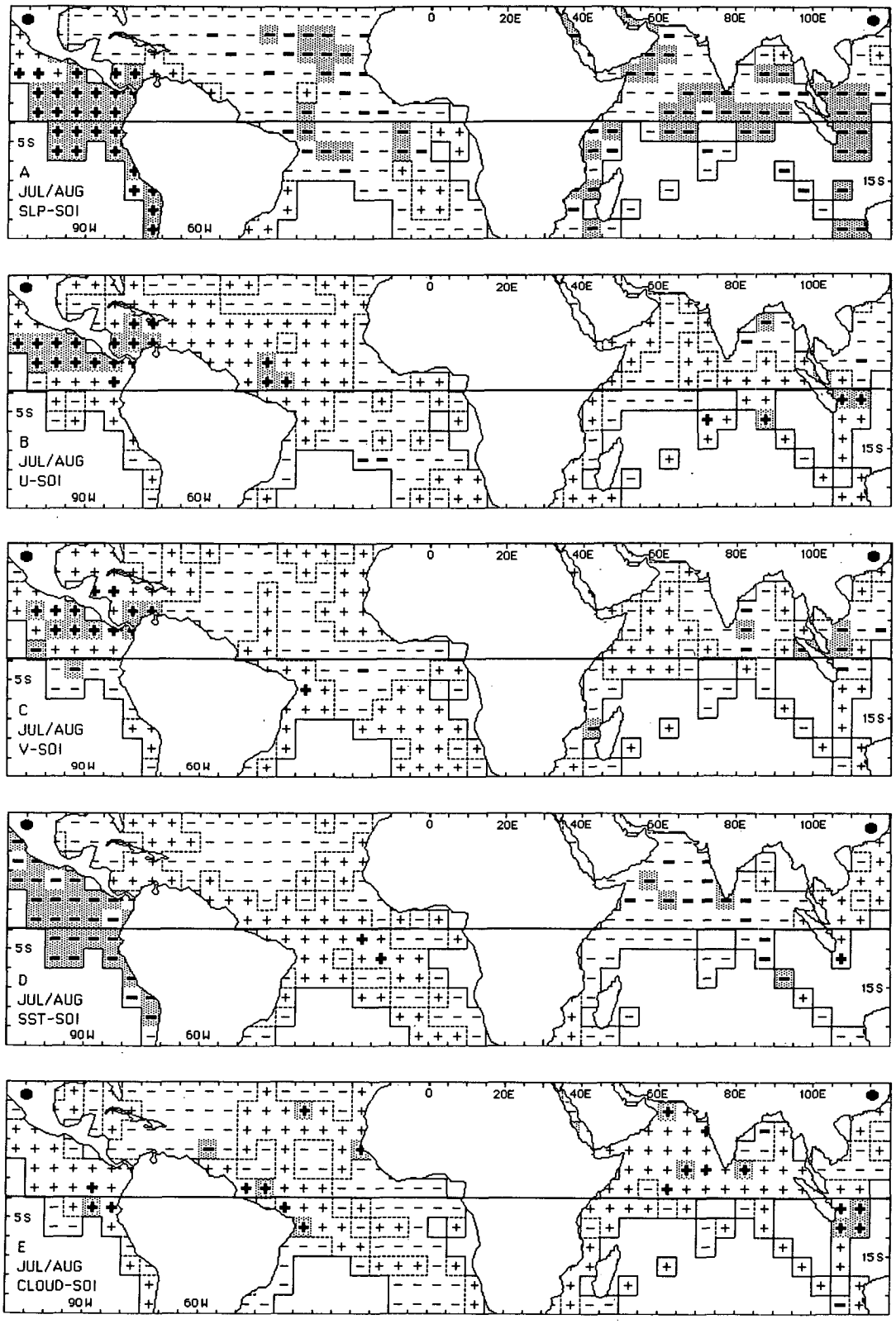

FIG. 6. As in Fig. 3 except for SOI, period 1948–83.

contains largely negative values. The pressure regression coefficient map (not shown here) displays lowest values in the Arabian Sea, tantamount to steepened northward pressure gradients in the western Indian Ocean. The u correlation map (Fig. 6b), which is not field significant, is indistinct, whereas the field significant v correlation map (Fig. 6c) contains positive values in the western Indian Ocean and strong negative correlations in the eastern Indian Ocean. The SST correlation map (Fig. 6d) is characterized by negative values and is field significant. The field significant CLOUD correlation map (Fig. 6e) contains mainly positive values throughout the Indian Ocean. The SOI correlation maps were also analyzed for the period 1948–72 and though fewer maps are field significant, the correlation patterns are quite similar.

In summary, the positive SO phase is characterized in the eastern Pacific by anomalously high pressure, reduced northeast trades, cool surface waters, and enhanced cloudiness; and in the Indian Ocean by anomalously low pressure, enhanced southerly flow in the western and diminished southerly flow in the eastern Indian Ocean, cool surface waters, and increased cloudiness. These results are consistent with various earlier studies [review in Hastenrath (1988, pp. 253–258)].

7. Conclusions

A host of empirical and modeling investigations over the past 15 years have served to demonstrate the great complexity of the Sahel drought problem. Thus, it is increasingly being recognized that both anthropogenic modifications of surface conditions in situ and large-scale circulation controls may be contributing factors, that both year-to-year and decadal scale variations in circulation and regional climate are important, and that seasonal evolutions of anomalous circulation regimes involve both atmosphere and ocean. In this context, the present study had limited objectives: it attempted to shed light on the diversity of circulation and climate anomalies in a band centered around 10–20°N and stretching from the Atlantic across Africa into the Indian Ocean sector, where rainfall is narrowly confined to the height of the boreal summer monsoon. The 1948–83 period analyzed here extends from an era of abundant precipitation into the most severe drought regime of the century, and features both interannual and trend-like variations. These components are not distinguished in the correlation analysis, and no attempt was made to trace the seasonal evolution of departure characteristics. Deliberately, work focused on the height of the rainy season, when zonal contrasts of climatic anomalies may be most clearly developed.

The hydrometeorological index series representative of large homogeneous regions within the monsoon belt (SENEGAL, SAHEL, ROSEIRES, ATBARA, NIR) indicate both spatial coherence and diversity of drought across this zone. The western Sahel (SENEGAL, SAHEL) varies largely in unison, as do the various hydrological catchments of the Nile basin (ROSEIRES, ATBARA); but the latter domain representing the eastern extremity of the Subsaharan zone has less in common with the rainfall anomalies of the western Sahel, and rather more with the vagaries in Indian monsoon rainfall (NIR). Likewise, the SO is strongly related to hydrometeorological anomalies in India and the Nile basin, but much less to those in the western Sahel.

Abundant rainfall in the western Sahel is associated in the Atlantic with weaker northeast trades, while low pressure and anomalously cold surface waters are found in the western Indian Ocean. In the eastern portion of the Subsaharan zone copious precipitation is accompanied by similar circulation departure characteristics in the tropical Atlantic sector, namely decreased northeast trades. More conspicuous, however, are the concomitant circulation anomalies in the Indian Ocean. These include anomalously low pressure, cool surface waters, and abundant cloudiness, particularly to the north of the equator. These alterations of the large-scale circulation setting are also typical of abundant Indian monsoon rainfall.

The SO is most clearly associated with the circulation departures in the Indian Ocean and rather less with those in the Atlantic. In this context, it is noteworthy that the SO is particularly strongly related to hydrometeorological anomalies in India and the Nile basin, and less so to those in the western Sahel. In the positive SO phase, when rainfall and water discharge tend to be abundant across the monsoon belt, especially its eastern portion, pressure tends to be low over both the tropical North Atlantic and the northern Indian oceans.

In conclusion, the present study reveals coherence but also remarkable differences of hydrometeorological anomalies across the monsoon belt. The western Sahel shows strongest associations with circulation departures in the tropical Atlantic. By contrast, the Nile discharge exhibits a remarkable affinity to Indian monsoon rainfall, and both are closely related to the circulation in the Indian Ocean sector. Inasmuch as the tropical Atlantic is regarded as a major moisture source also for the eastern part of the Subsaharan zone, it appears that the discharge fluctuations in the Nile basin may be related to variations in the Indian Ocean sector through other dynamical factors, such as the large-scale vertical motion field. It is intended to explore these and other issues raised by the present investigation through judicious general circulation model experiments and case studies of upper-air circulation.

Acknowledgments. This paper stems from an M.S. thesis in the Department of Meteorology, University of Wisconsin, Madison, under the guidance of Professor Stefan Hastenrath. The study was supported by NSF Grant ATM-8722410, NOAA Grant NA86AA-

D-AC064, and a Patricia Roberts Harris fellowship. For constructive criticism I thank Professors John Anderson and John Kutzbach, Dr. Leonard Druyan, and an anonymous reviewer.

REFERENCES

Abramowitz, M., and I. A. Stegun, Eds., 1964: *Handbook of Mathematical Functions with Formulas, Graphs, and Mathematical Tables.* Wiley, 1046 pp.

Charney, J. G., 1975: Dynamics of deserts and drought in the Sahel. *Quart. J. Roy. Meteor Soc.,* **101,** 193–202.

Druyan, L. M., 1987: GCM studies of the African summer monsoon. *Climate Dynamics,* **2,** 117–126.

——, 1988: SST-Sahel drought teleconnections in GCM simulations. *Recent Climatic Change,* Gregory, S., Ed., Bellhaven Press, 154–165.

——, 1989: Advances in the study of sub-Saharan drought. *Int. J. Climatol.,* **9,** 77–90.

Folland, C. K., T. N. Palmer, and D. E. Parker, 1986: Sahel rainfall and worldwide sea temperatures, 1905–85. *Nature,* **320,** 602–607.

Hastenrath, S., 1976: Variations in low-latitude circulation and extreme climatic events in the tropical Americas. *J. Atmos. Sci.,* **33,** 202–215.

——, 1988: *Climate and Circulation of the Tropics.* Reidel, 455 pp.

——, and P. J. Lamb, 1977: *Climatic Atlas of the Tropical Atlantic and Eastern Pacific Oceans.* University of Wisconsin Press, 113 pp.

——, and ——, 1978: *Heat Budget Atlas of the Tropical Atlantic and Eastern Pacific Oceans.* University of Wisconsin Press, 103 pp.

——, and ——, 1979: *Climatic Atlas of the Indian Ocean.* University of Wisconsin Press, 203 pp.

——, L. C. Castro and P. Aceituno, 1987: The Southern Oscillation in the tropical sector. *Contrib. Atmos. Phys.,* **60,** 447–63.

Kutzbach, J. E., 1987: The changing pulse of the monsoon. *Monsoons,* J. S. Fein and P. L. Stephens, Eds., Wiley, 247–268.

Lamb, P. J., 1978a: Case studies of tropical Atlantic surface circulation patterns during recent sub-Saharan weather anomalies: 1967 and 1968. *Mon. Wea. Rev.,* **106,** 482–491.

——, 1978b: Large-scale tropical Atlantic surface circulation patterns associated with Subsaharan weather anomalies. *Tellus,* **30,** 240–251.

——, 1985: Rainfall in Subsaharan West Africa during 1941–83. *Zeitschrift für Gletscherkunde und Glazialgeologie,* **21,** 131–139.

Livezey, R. E., and W. Y. Chen, 1983: Statistical field significance and its determination by Monte Carlo techniques. *Mon. Wea. Rev.,* **111,** 46–59.

Lough, J. M., 1986: Tropical Atlantic sea surface temperatures and rainfall variations in Subsaharan Africa. *Mon. Wea. Rev.,* **114,** 561–570.

Mooley, D. A., and B. Parthasarathy, 1984: Fluctuations in all-India summer monsoon rainfall during 1871–1978. *Climatic Change,* **6,** 287–301.

Nicholson, S. E., 1985: Sub-Saharan rainfall 1981–84. *J. Climate Appl. Meteor.,* **24,** 1388–1391.

Oort, A. H., Y. H. Pan, R. W. Reynolds, and C. F. Ropelewski, 1987: Historical trends in the surface temperature over the oceans based on the COADS. *Climate Dyn.,* **2,** 29–38.

Owen, J. A., and C. K. Folland, 1988: Modelling the influence of sea surface temperatures on tropical rainfall. *Recent Climatic Change,* Gregory, S., Ed., Bellhaven Press, 141–153.

Palmer, T. N., 1986: Influence of the Atlantic, Pacific and Indian Oceans on Sahel rainfall. *Nature,* **322,** 251–253.

Quenouille, M. H., 1952: *Associated Measurements.* Butterworths, 242 pp.

Ropelewski, C. F., and M. S. Halpert, 1989: Precipitation patterns associated with the high index phase of the Southern Oscillation. *J. Climate,* **2,** 268–284.

Shahin, M., 1985: *Hydrology of the Nile Basin.* Elsevier, 575 pp.

Wolter, K., 1989: Modes of tropical circulation, Southern Oscillation, and Sahel rainfall anomalies. *J. Climate,* **2,** 149–172.